A new Abel inversion by means of the integrals of an input function with noise

2007 J. Phys. A: Math. Theor. 40 347

(http://iopscience.iop.org/1751-8121/40/2/012)

INSTITUTE OF PHYSICS PUBLISHING JOURNAL OF PHYSICS A: MATHEMATICAL AND THEORETICAL

J. Phys. A: Math. Theor. **40** (2007) 347–360 doi:10.1088/1751-8113/40/2/012

A new Abel inversion by means of the integrals of an input function with noise

Xian-Fang Li[1], Li Huang[2] and Yong Huang[2]

[1] Institute of Mechanics and Sensor Technology, School of Civil Engineering and Architecture, Central South University, Changsha, Hunan 410083, People's Republic of China
[2] College of Mathematics and Computer Science, Hunan Normal University, Changsha 410081, People's Republic of China

E-mail: xfli@mail.csu.edu.cn

Received 25 October 2006
Published 12 December 2006
Online at stacks.iop.org/JPhysA/40/347

Abstract

Abel's integral equations arise in many areas of natural science and engineering, particularly in plasma diagnostics. This paper proposes a new and effective approximation of the inversion of Abel transform. This algorithm can be simply implemented by symbolic computation, and moreover an nth-order approximation reduces to the exact solution when it is a polynomial in r^2 of degree less than or equal to n. Approximate Abel inversion is expressed in terms of integrals of input measurement data; so the suggested approach is stable for experimental data with random noise. An error analysis of the approximation of Abel inversion is given. Finally, several test examples used frequently in plasma diagnostics are given to illustrate the effectiveness and stability of this method.

PACS numbers: 52.70.−m, 02.30.Zz

(Some figures in this article are in colour only in the electronic version)

1. Introduction

Abel's integral equations are frequently encountered in a variety of physical problems and engineering applications such as geophysics [1], astrophysics [2], ocean acoustic tomography [3], radio science [4], image reconstruction [5], optics [6] and so on. In particular, in flame and plasma diagnostics [7], the radial profile of the plasma emission coefficient or electron density can be reconstructed from measured radiation intensity or integrated phase shifts.

Usually, the plasma is assumed to be optically thin, and has a cylindrical symmetry. Under such circumstances, the measured intensity of radiation $I(y)$ is related to the emission coefficient $g(r)$ of light source with radial distribution according to an integral over a line-of-sight chord or Abel transform

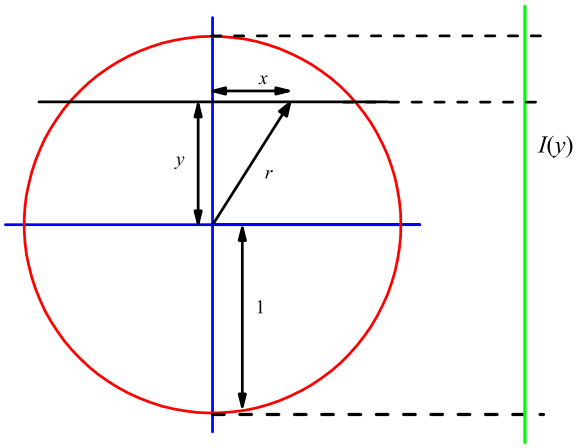

Figure 1. Schematic of a geometry of a cylindrically symmetric radiation source and the corresponding coordinates.

$$I(y) = \int_{-\sqrt{1-y^2}}^{\sqrt{1-y^2}} g(r)\,\mathrm{d}x = 2\int_{y}^{1} \frac{g(r)r}{\sqrt{r^2-y^2}}\,\mathrm{d}r, \tag{1}$$

where y is the position of a chord from the plasma centre, $r(r^2 = x^2 + y^2)$ the radial distance from the plasma centre, as shown in figure 1. Here $I(1) = 0$ is a boundary condition based on consideration of physical backgrounds of discrete problems, and the radius of the plasma cylinder is normalized to unity.

Knowledge of an exact analytical form of $I(y)$ can directly give Abel inversion as follows:

$$g(r) = -\frac{1}{\pi}\int_{r}^{1} \frac{I'(y)}{\sqrt{y^2-r^2}}\,\mathrm{d}y, \tag{2}$$

where $I'(y) = \mathrm{d}I/\mathrm{d}y$ is the derivative of $I(y)$ with respect to y. However, unfortunately this Abel inversion fails in practical applications. The reason is that the derivative involved is ill-posed, and severely amplifies errors because $I(y)$ is, in effect, given at some discrete positions through experimental observation data with inevitable measurement errors. To overcome this drawback, it is therefore most desirable to obtain an accurate, stable and fast method for computing Abel inversion, and to date many methods have been proposed for this purpose.

One approach is to employ the curve fitting techniques such as the least-squares polynomial fit [8–10], which are able to affect the true curve due to the treatment of smoothing experimental data. Another approach is to expand the desired inverse with respect to a chosen basis including various orthogonal polynomials [11, 12], and then determine coefficients by inserting the expansion into Abel's integral equations. Based on the integral transform methods, Abel's integral equations can be converted to computing two infinite integrals involving a Bessel function [13–15]. In addition, a conventional slice-and-stack method [16] and its modification [17] have also been set forth. On the other hand, by integration by parts or some manipulations, Abel inversion can be transformed to a form of derivative-free integral, but the integral involved is related to higher order singularity [18, 19]. Just pointed out in [20], the explicit differentiation in the standard inversion is obviated, but the derived formulae are in fact equivalent to a half-differentiation and also ill-posed. The above-mentioned methods can be categorized into two classes: one using analytical expressions [21, 22] and the other mainly depending on numerical techniques [23, 24].

In this study, we present a novel, simple, fast and efficient approach for solving approximate inversion of Abel transform. The obtained formula is given in terms of the integrals of input measured radiation intensity $I(y)$, so that amplification of measurement errors can be efficiently avoided. Moreover, the resulting approximation of Abel inversion can be simply performed by symbolic computation at any personal computer. Also, the nth-order approximation $g_n(r)$ of Abel inversion is identical to the exact noise-free emission coefficient $g(r)$ when $g(r)$ is a polynomial in r^2 of degree n. Error of approximate Abel inversion is analysed. Finally, test examples turn out that this method is quite stable without resort to other data-smoothing techniques.

2. Method

Due to symmetry of the problem in question, $g(r)$ is even with respect to r and we expand $g(r)$ as a generalized Taylor–Stieltjes polynomial in r^2 with a remainder, i.e.,

$$g(r) = g(y) + \sum_{j=1}^{n} \frac{g_\beta^{(j)}(y)}{j!}(r^2 - y^2)^j + \frac{g_\beta^{(n+1)}(\xi)}{(n+1)!}(r^2 - y^2)^{n+1}, \tag{3}$$

where ξ denotes a point between r and y, and $g'_\beta(y)$ stands for the first-order Stieltjes derivative of $g(y)$, defined by [25]

$$g'_\beta(y_0) = \lim_{y \to y_0} \frac{g(y) - g(y_0)}{y^2 - y_0^2}, \tag{4}$$

and higher order Stieltjes derivatives $g_\beta^{(j)}(y)(j \geqslant 2)$ are similarly defined as

$$g_\beta^{(j+1)}(y_0) = \lim_{y \to y_0} \frac{g_\beta^{(j)}(y) - g_\beta^{(j)}(y_0)}{y^2 - y_0^2}. \tag{5}$$

If $g_\beta^{(n+1)}(y)$ is bounded, the last remainder term is sufficiently small for an enough large n. In practical applications, this condition is readily satisfied. Therefore, in what follows we neglect this remainder term, and approximate $g(r)$ as

$$g(r) \approx g(y) + \sum_{j=1}^{n} \frac{g_\beta^{(j)}(y)}{j!}(r^2 - y^2)^j. \tag{6}$$

It is worth noting that the above nth-order approximation is exact for a polynomial in r^2 of degree equal to or less than n.

Substituting (6) for $g(r)$ into equation (1), one can get

$$I(y) = 2\int_y^1 \frac{r}{\sqrt{r^2 - y^2}} \left[g(y) + \sum_{j=1}^{n} \frac{g_\beta^{(j)}(y)}{j!}(r^2 - y^2)^j \right] \mathrm{d}r, \tag{7}$$

or further

$$I(y) = \sum_{j=0}^{n} \frac{g_\beta^{(j)}(y)}{j!(j+0.5)}(1 - y^2)^{j+0.5}, \tag{8}$$

where

$$g_\beta^{(0)}(y) = g(y).$$

We take $g(y), g'_\beta(y), \ldots, g_\beta^{(n)}(y)$ as $n+1$ independent unknowns. In order to determine them, we still need n other independent linear equations, and $g(y), g'_\beta(y), \ldots, g_\beta^{(n)}(y)$ are

therefore determined by solving a system of linear equations for them. This can be achieved by multiplying both sides of equation (1) by y and integrating both sides of equation (1) with respect to y from x to 1. Accordingly, we get that

$$\int_x^1 yI(y)\,\mathrm{d}y = 2\int_x^1 y\int_y^1 \frac{rg(r)}{\sqrt{r^2-y^2}}\,\mathrm{d}r\,\mathrm{d}y. \tag{9}$$

Changing the order of the integration on the right-hand side of equation (9), we have

$$\int_y^1 rI(r)\,\mathrm{d}r = 2\int_y^1 rg(r)\sqrt{r^2-y^2}\,\mathrm{d}r, \tag{10}$$

where we have replaced variable x with y in the last step of above derivation, for convenience.

Applying Taylor–Stieltjes expansion again and substituting (6) for $g(r)$ into equation (10) gives

$$\int_y^1 rI(r)\,\mathrm{d}r = 2\int_y^1 r\sqrt{r^2-y^2}\left[g(y)+\sum_{j=1}^{n}\frac{g_\beta^{(j)}(y)}{j!}(r^2-y^2)^j\right]\mathrm{d}r, \tag{11}$$

or

$$\int_y^1 rI(r)\,\mathrm{d}r = \sum_{j=0}^{n}\frac{g_\beta^{(j)}(y)}{j!(j+1.5)}(1-y^2)^{j+1.5}. \tag{12}$$

Now we have arrived at another linear equation for $g(y), g'_\beta(y), \ldots, g_\beta^{(n)}(y)$. By repeating the above integration process for $n-1$ times, one can arrive at

$$\frac{1}{(i-1)!}\int_y^1 rI(r)(r^2-y^2)^{i-1}\,\mathrm{d}r = \frac{2^i}{(2i-1)!!}\int_y^1 rg(r)(r^2-y^2)^{i-0.5}\,\mathrm{d}r,$$
$$i=2,3,\ldots,n. \tag{13}$$

Putting (6) for $g(r)$ into the above equation yields

$$\int_y^1 r(r^2-y^2)^{i-1}I(r)\,\mathrm{d}r = \frac{(2i-2)!!}{(2i-1)!!}\sum_{j=0}^{n}\frac{g_\beta^{(j)}(y)}{j!(i+j+0.5)}(1-y^2)^{i+j+0.5},$$
$$i=2,3,\ldots,n. \tag{14}$$

Therefore, equations (8), (12) and (14) form a systems of $n+1$ linear equations for $n+1$ unknowns $g_\beta^{(j)}(y)(j=0,1,\ldots,n)$, which can be rewritten in a compact form as

$$\mathbf{A}_{nn}\mathbf{G}_n = \mathbf{b}_n, \tag{15}$$

with

$$\mathbf{A}_{nn} = (a_{ij}(y))_{(n+1)\times(n+1)}, \qquad \mathbf{G}_n = \left(\frac{g_\beta^{(i)}(y)}{i!}\right)_{(n+1)\times 1}, \qquad \mathbf{b}_n = (b_i(y))_{(n+1)\times 1}, \tag{16}$$

where

$$a_{ij}(y) = \begin{cases} \dfrac{(1-y^2)^{j+0.5}}{j+0.5}, & i=0, \quad 0\leqslant j\leqslant n, \\ \dfrac{(2i-2)!!}{(2i-1)!!}\dfrac{(1-y^2)^{i+j+0.5}}{(i+j+0.5)}, & i>0, \quad 0\leqslant j\leqslant n, \end{cases} \tag{17}$$

$$b_i(y) = \begin{cases} I(y), & i=0, \\ \displaystyle\int_y^1 r(r^2-y^2)^{i-1}I(r)\,\mathrm{d}r, & 1\leqslant i\leqslant n. \end{cases} \tag{18}$$

Introducing

$$\mathbf{C}_{nn}(x) = \begin{bmatrix} \frac{1}{x} & \frac{1}{x+1} & \cdots & \frac{1}{x+n} \\ \frac{1}{x+1} & \frac{1}{x+2} & \cdots & \frac{1}{x+1+n} \\ \vdots & \vdots & \ddots & \vdots \\ \frac{1}{x+n} & \frac{1}{x+n+1} & \cdots & \frac{1}{x+2n} \end{bmatrix}, \tag{19}$$

it is easily verified that $\det(\mathbf{C}_{nn}(x)) \neq 0$ for any positive x, the proof of which is given in the appendix. Furthermore, one can get

$$\det(\mathbf{A}_{nn}) = u^{(n+1)(2n+1)} \det(\mathbf{C}_{nn}(0.5)) \prod_{i=1}^{n} \frac{(2i-2)!!}{(2i-1)!!}, \tag{20}$$

and so $\det(\mathbf{A}_{nn}) \neq 0$. Here and hereinafter, we denote

$$u = \sqrt{1-y^2}. \tag{21}$$

By using the well-known Cramer's rule, one immediately finds that the solution to equation (15) can be determined. In particular, we obtain the nth-order approximation of the exact solution to equation (1) denoted as $g_n(y)$ as follows:

$$g_n(y) = \frac{1}{u \det(\mathbf{C}_{nn}(0.5))} \begin{vmatrix} I(y) & \frac{1}{1.5} & \cdots & \frac{1}{n+0.5} \\ u^{-2}b_1(y) & \frac{1}{2.5} & \cdots & \frac{1}{n+1.5} \\ \vdots & \vdots & \ddots & \vdots \\ \frac{(2n-1)!!}{(2n-2)!!}u^{-2n}b_n(y) & \frac{1}{n+1.5} & \cdots & \frac{1}{2n+0.5} \end{vmatrix}. \tag{22}$$

Moreover, this nth-order approximation is exact for a solution of polynomial in y^2 of degree equal to or less than n.

3. Error analysis

To give an error analysis of the above-derived approximation, let us assume that the exact solution to be determined is infinitely differentiable with respect to r^2. In other words, we can write

$$g(r) = g(y) + \sum_{j=1}^{\infty} \frac{g_\beta^{(j)}(y)}{j!}(r^2-y^2)^j. \tag{23}$$

Furthermore, generalized Taylor–Stieltjes derivatives of any order, $g_\beta^{(j)}(y)$, of $g(y)$ are assumed to be continuous and bounded in an interval of interest. Or rather, there exists a positive constant C_n such that

$$\left|g_\beta^{(j)}(y)\right| \leqslant C_n, \qquad j \geqslant n. \tag{24}$$

Clearly, the following relations

$$C_0 \geqslant C_1 \geqslant \cdots \geqslant C_n \geqslant \cdots \tag{25}$$

hold. For convenience, we denote this class of such functions g as C_β^∞.

Similar to the preceding treatment, Abel's integral equation can be transformed to the following equivalent infinitely linear system of unknown $g_\beta^{(j)}(y)$, $j = 0, 1, \ldots,$

$$\mathbf{AG} = \mathbf{b}, \tag{26}$$

with

$$\mathbf{A} = \lim_{n\to\infty} \mathbf{A}_{nn}, \qquad \mathbf{G} = \lim_{n\to\infty} \mathbf{G}_n, \qquad \mathbf{b} = \lim_{n\to\infty} \mathbf{b}_n, \tag{27}$$

where $\mathbf{A}_{nn}$, $\mathbf{G}_n$ and $\mathbf{b}_n$ are defined as before.

To evaluate the difference between the solutions to equations (15) and (26), following Ursell [26] we also rewrite equation (15) as an infinite linear system of the form

$$\mathbf{A}^*\mathbf{G}^* = \mathbf{b}^* \tag{28}$$

such that

$$\mathbf{A}^* = \begin{pmatrix} \mathbf{A}_{nn} & \mathbf{0}_{n\infty} \\ \mathbf{0}_{\infty n} & \mathbf{U}_{\infty\infty} \end{pmatrix}, \qquad \mathbf{G}^* = \begin{pmatrix} \mathbf{G}_n \\ \widetilde{\mathbf{G}} \end{pmatrix}, \qquad \mathbf{b}^* = \begin{pmatrix} \mathbf{b}_n \\ \widetilde{\mathbf{b}} \end{pmatrix}, \tag{29}$$

where $\mathbf{0}_{n\infty}$ and $\mathbf{0}_{\infty n}$ stand for zero matrices with infinite columns and infinite rows, respectively, $\mathbf{U}_{\infty\infty}$ the infinite unity matrix, $\widetilde{\mathbf{G}}$ and $\widetilde{\mathbf{b}}$ are relevant functions. If denoting $\mathbf{M} = \mathbf{A} - \mathbf{A}^*$, one gets

$$\mathbf{M} = \begin{pmatrix} \mathbf{0}_{nn} & \mathbf{A}_{n\infty} \\ \mathbf{A}_{\infty n} & \mathbf{M}_{\infty\infty} \end{pmatrix}. \tag{30}$$

Now, considering (27) we take $\mathbf{b}^* = \mathbf{b}$, corresponding to an input function without noise, and subtract (28) from (26), yielding

$$\mathbf{AG} - \mathbf{A}^*\mathbf{G}^* = 0, \tag{31}$$

which can be further rewritten as

$$\mathbf{A}^*(\mathbf{G} - \mathbf{G}^*) = -(\mathbf{A} - \mathbf{A}^*)\mathbf{G}. \tag{32}$$

Taking into account that $\mathbf{A}_{nn}$ is non-singular, and so is $\mathbf{A}^*$, from the above equation one can find

$$\mathbf{G} - \mathbf{G}^* = -(\mathbf{A}^*)^{-1}(\mathbf{A} - \mathbf{A}^*)\mathbf{G}, \tag{33}$$

which further allows us to derive

$$\mathbf{G} - \mathbf{G}^* = -\begin{pmatrix} \mathbf{0}_{nn} & \mathbf{A}_{nn}^{-1}\mathbf{A}_{n\infty} \\ \mathbf{A}_{\infty n} & \mathbf{M}_{\infty\infty} \end{pmatrix}\mathbf{G}. \tag{34}$$

Introducing

$$\mathbf{H} = \mathbf{A}_{nn}^{-1}\mathbf{A}_{n\infty} = (h_{ij})_{n\times\infty}, \text{ say,}$$

remembering (16) and (27) we get the first element of the vector on the left-hand side of (34) expressed by

$$g(y) - g_n(y) = -\sum_{j=0}^{\infty} \frac{h_{0j}}{(j+n+1)!} g_\beta^{(j+n+1)}(y). \tag{35}$$

Therefore, in view of (24), we immediately get an error of the nth-order approximation as

$$|g(y) - g_n(y)| \leqslant \frac{eC_{n+1}}{(n+1)!} \max_{j\geqslant 0}(|h_{0j}|) \leqslant \frac{eC_0}{(n+1)!} \max_{j\geqslant 0}(|h_{0j}|). \tag{36}$$

In particular, if the exact solution $g(y)$ is a polynomial in y^2 of degree equal to or less than n, then $C_{n+1} = 0$ can be derived, which means that the exact solution $g(y)$ is identical to the nth-order approximation $g_n(y)$, i.e.

$$g(y) = g_n(y). \tag{37}$$

Next, let us consider the case of an input function with noise. In this case, we take

$$\mathbf{b}^* = \mathbf{b} + \varepsilon, \tag{38}$$

with

$$\varepsilon = \begin{pmatrix} \varepsilon(y) \\ \int_y^1 r\varepsilon(r)\,\mathrm{d}r \\ \vdots \\ \int_y^1 r(r^2 - y^2)^{i-1}\varepsilon(r)\,\mathrm{d}r \\ \vdots \end{pmatrix}, \tag{39}$$

where $\varepsilon(y)$ denotes random noise. From the above, other elements are clearly expressed by the integrals of $\varepsilon(y)$.

In a similar fashion, by subtracting (28) from (26), one obtains

$$\mathbf{AG} - \mathbf{A}^*\mathbf{G}^* = -\varepsilon, \tag{40}$$

from which one further gets

$$\mathbf{G}^* - \mathbf{G} = \begin{pmatrix} \mathbf{0}_{nn} & \mathbf{A}_{nn}^{-1}\mathbf{A}_{n\infty} \\ \mathbf{A}_{\infty n} & \mathbf{M}_{\infty\infty} \end{pmatrix} \mathbf{G} + \begin{pmatrix} \mathbf{A}_{nn}^{-1} & \mathbf{0}_{n\infty} \\ \mathbf{0}_{\infty n} & \mathbf{U}_{\infty\infty} \end{pmatrix} \varepsilon. \tag{41}$$

Obviously, the first part of the right-hand side corresponds to the error between the exact solution and the nth-order approximation in the absence of noise, and the second part describes the error induced by random noise. Restricting our attention to the first element of $\mathbf{G}^* - \mathbf{G}$ gives a desired accuracy of the approximate Abel inversion in the presence of noise.

Note that although the function $g(r)$ considered in this section is assumed to be even and infinitely differentiable with respect to r^2, practical application to be given in the following section indicates that such a constraint can be further relaxed. The present method is also suitable for a function with odd power, a piecewise function, and a non-polynomial function.

4. Test examples

In this section, to examine the effectiveness of the suggested method, several test examples used frequently in plasma diagnostics to assess the performance of Abel inversion are given as follows

Example 1 [10, 27, 29]

$$g(r) = \tfrac{1}{2}(1 + 10r^2 - 23r^4 + 12r^6),$$
$$I(y) = \tfrac{8}{105}u(19 + 34y^2 - 125y^4 + 72y^6).$$

Example 2 [12, 13, 19, 21, 22, 28, 29]

$$g(r) = \begin{cases} 1 - 2r^2, & 0 \leqslant r \leqslant 0.5, \\ 2(1 - r)^2, & 0.5 < r \leqslant 1, \end{cases}$$

$$I(y) = \begin{cases} \dfrac{4u}{3}(1 + 2y^2) - \dfrac{2v}{3}(1 + 8y^2) - 4y^2 \ln\dfrac{1+u}{0.5+v}, & 0 \leqslant r \leqslant 0.5, \\ \dfrac{4}{3}(1 + 2y^2)u - 4y^2 \ln\dfrac{1+u}{y}, & 0.5 < r \leqslant 1. \end{cases}$$

Example 3 [12, 27, 29]

$$g(r) = (1-r^2)^{-3/2}\exp\left[1.1^2\left(1-\frac{1}{1-r^2}\right)\right],$$
$$I(y) = \frac{\sqrt{\pi}}{1.1u}\exp\left[1.1^2\left(1-\frac{1}{1-y^2}\right)\right].$$

Example 4 [15, 24, 29]

$$g(r) = \begin{cases} 0.1 + 5.51r - 5.25r^3, & 0 \leqslant r \leqslant 0.7, \\ -40.74 + 155.56r - 188.89r^2 + 74.07r^3, & 0.7 < r \leqslant 1, \end{cases}$$
$$I(y) = \begin{cases} 22.68862u^* + 217.557u^*y^2 - 59.49y^4 \ln\dfrac{0.7+u^*}{y} + I^*(y), & 0 \leqslant r \leqslant 0.7, \\ I^*(y), & 0.7 < r \leqslant 1, \end{cases}$$

with

$$I^*(y) = -14.811\,667u - 196.300\,83uy^2 + y^2\left(155.56\ln\frac{1+u}{0.7+u^*} + 55.5525y^2\ln\frac{1+u}{y}\right).$$

Example 5 [29, 30]

$$g(r) = 1 - 3r^2 + 2r^3,$$
$$I(y) = u\left(1-\frac{5}{2}y^2\right) + \frac{3}{2}y^4\ln\frac{1+u}{y}.$$

In the above examples $u = \sqrt{1-y^2}$, $u^* = \sqrt{0.7^2 - y^2}$, $v = \sqrt{(1-4y^2)/4}$. It is noted that in the fourth example, two misprints in the expression for $I(y)$ given in [29] have been corrected.

In the above examples, the emission coefficient $g(r)$ in the first example is an even function, and has off axis peak. For this example, we find that the reconstruction $g_n(r)$ of $g(r)$ when $n \geqslant 3$ is identical to the exact emission coefficient $g(r)$, which implies the effectiveness of this method. Moreover, by symbolic computation, the derived reconstruction $g_3(r) \equiv g(r)$ due to $g(r)$ being a polynomial in r^2 of degree 3, as expected. The emission coefficient $g(r)$ in example 5 is an odd function having cubic dependence, and the remaining three examples are not usual polynomials, standing for various profiles of the emission coefficient. The profiles of all five emission coefficients are displayed in figure 2. Due to $g(r)$ not being a polynomial in r^2, unlike example 1, the true $g(r)$ for the last four examples cannot be reconstructed exactly. Even this, we still can adopt the present method to reconstruct $g(r)$ to a satisfactory accuracy.

In what follows, a unity interval is partitioned into N equally spaced subintervals. To examine the accuracy and efficiency of the above results, we define the root mean square error and the relative residual by

$$\sigma_n = \sqrt{\frac{1}{N}\sum_{j=0}^{N-1}[g_n(r_j) - g(r_j)]^2}, \tag{42}$$
$$\Delta_n = \frac{\sum_{j=0}^{N-1}|g_n(r_j) - g(r_j)|}{\sum_{j=0}^{N-1} g(r_j)} \tag{43}$$

respectively, $g_n(r_j)$ and $g(r_j)$ being the reconstructed emission coefficients and the corresponding exact emission coefficients at N discrete positions, respectively. Note that

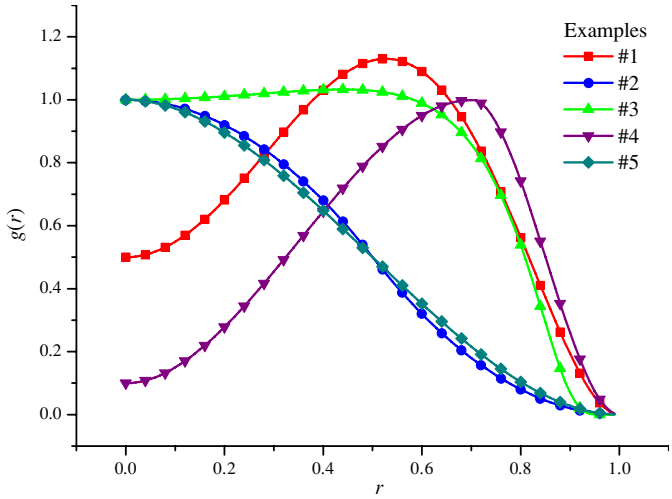

Figure 2. The theoretical values of the emission coefficient $g(r)$ of four examples considered.

Table 1. σ_n and Δ_n of four examples without noise with $N = 30$.

	Example 1		Example 2		Example 3		Example 4		Example 5	
n	σ_n	Δ_n	σ_n	Δ_n	σ_n	Δ_n	σ_n	Δ_n	σ_n	Δ_n
2	0.0777	0.084	0.0068	0.0100	0.0290	0.0286	0.0323	0.0524	0.0091	0.0121
3	0	0	0.0076	0.0100	0.0271	0.0276	0.0205	0.0305	0.0028	0.0032
4	0	0	0.0029	0.0039	0.0086	0.0084	0.0151	0.0209	0.0012	0.0012
5	0	0	0.0014	0.0017	0.0044	0.0045	0.0056	0.0081	0.0006	0.0006

$g_n(1) = 0$ can be deduced provided $I(y) = o(u)$ as $y \to 1$; consequently $g_n(r_N) = g(r_N) = 0$ at $r_N = 1$, removed from (42) and (43), for the practical case $I(1) = 0$.

In our computations, we first take $n = 2, 3, 4, 5$ and perform Abel inversion without any noisy input. Evaluated results of the root mean square error and the relative residual are tabulated in table 1. From table 1, σ_n and Δ_n decrease with n increasing except for example 2 when $n = 3$. Nevertheless, for the latter case the maximum absolute errors indeed decrease as n is raised. To manifest the discrepancy of the theoretical true values and the evaluated values, a difference between the exact $g(r)$ and the nth approximation $g_n(r)$, $g_n(r) - g(r)$, is shown for several lower n for example 2 in figure 3. Clearly, from figure 3 it is seen that with n increasing, the maximum absolute errors remarkably decrease. It should be noted that although $g(r)$ is not infinitely differentiable at $r = 0.5$ for example 2 and $r = 0.7$ for example 4, respectively, the present method is still efficient.

On the other hand, we find that when N takes a larger value, the accuracy of the evaluated results cannot be improved evidently. For example, for example 3 we get $\sigma_3 = 0.0268$, $\Delta_3 = 0.0275$ when taking $N = 100$ and $\sigma_3 = 0.0267$, $\Delta_3 = 0.0274$ when taking $N = 300$. Such a conclusion is due to the fact that the reconstructed $g_n(r)$ is determined analytically, directly dependent on n and not on N. The contribution of N only occurs in transforming the integrals appearing in $b_i(y)$ in (22) to a finite summation. In other words, once a smaller N gives an enough accurate result of integrals in (18) relative to $b_i(y)$, another larger N does not remarkably improve the accuracy of the numerical evaluation of integrals. Of

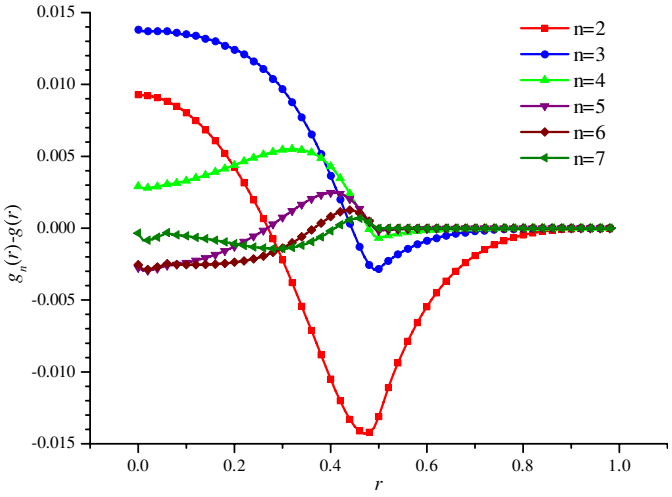

Figure 3. Difference between the exact emission coefficient $g(r)$ with its reconstruction $g_n(r)$ for example 2.

Table 2. σ_n and Δ_n of four examples with noise (case A) with $N = 30$.

	Example 1		Example 2		Example 3		Example 4		Example 5	
n	σ_n	Δ_n	σ_n	Δ_n	σ_n	Δ_n	σ_n	Δ_n	σ_n	Δ_n
2	0.0799	0.0867	0.0074	0.0121	0.0298	0.0299	0.0336	0.0543	0.0111	0.0195
3	0.0077	0.0085	0.0084	0.0131	0.0283	0.0293	0.0228	0.0344	0.0091	0.0151
4	0.0092	0.0096	0.0079	0.0131	0.0131	0.0132	0.0185	0.0261	0.0106	0.0178
5	0.0121	0.0121	0.0101	0.0155	0.0115	0.0113	0.0119	0.0182	0.0136	0.0218

course, σ_n and Δ_n drop only if the order of approximation increases. This feature is different from that via numerical techniques for determining Abel inversion [15]. For the latter case, N is often required larger than 100 [29] so that $\Delta_n < 0.01$. In the following computations, for simplicity we take $N = 30$.

To simulate true measurement data with random noise, we take measured radiation intensity as $I_\varepsilon(y)$ instead of $I(y)$, and two different cases are analysed. Case A corresponds to $I_\varepsilon(y)$ consisting of the same $I(y)$ values rounded off to the second decimal place, and case B to $I_\varepsilon(y) = I(y)[1 + \varepsilon_0\theta(y)]$, where ε_0 is a small constant and $\theta(y)$ denotes a uniform random variable with values in $[-1, 1]$, which can be generated by a computer based on random-number generator at discrete N positions. Furthermore, we employ cubic spline function to fit $I_\varepsilon(y)$ to guarantee a smooth curve, and then using this curve or its values at certain positions, calculate integrals in Abel inversion given by (22). For case A, evaluated σ_n and Δ_n are listed in table 2. From table 2, it is observed that the obtained results are still reasonable in the presence of noise. In particular, with an increase of n, σ_n and Δ_n decline for examples 3 and 4. In contrast, when n arrives at a so-called optimal value, $n = 3$ for examples 1 and 5 and $n = 4$ for example 2, σ_n and Δ_n slightly rise if n continues to increase. This phenomenon is similar to that in [29], and however, the order n of approximation $g_n(r)$ here is much less than the order of fitting polynomial in [29]. Additionally, from the results of example 2 in table 2, one can see that the accuracy based on the present method is higher than that of [19] where

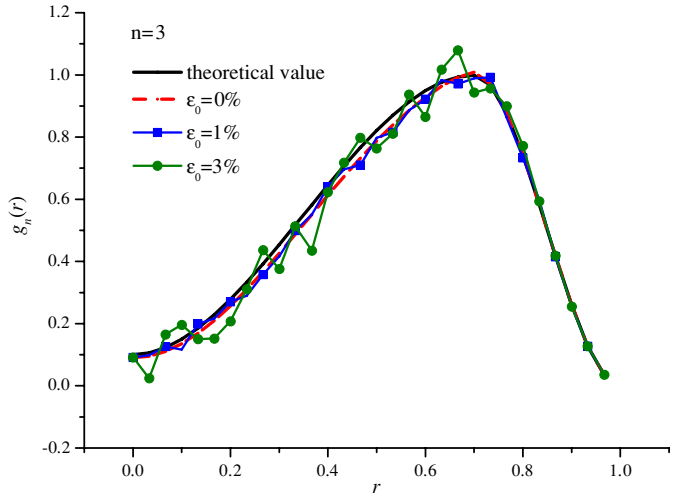

Figure 4. Comparison of the exact emission coefficient $g(r)$ with its three-order reconstruction $g_3(r)$ for example 4 (case B) with $\varepsilon_0 = 0\%, 1\%, 3\%$ added noise.

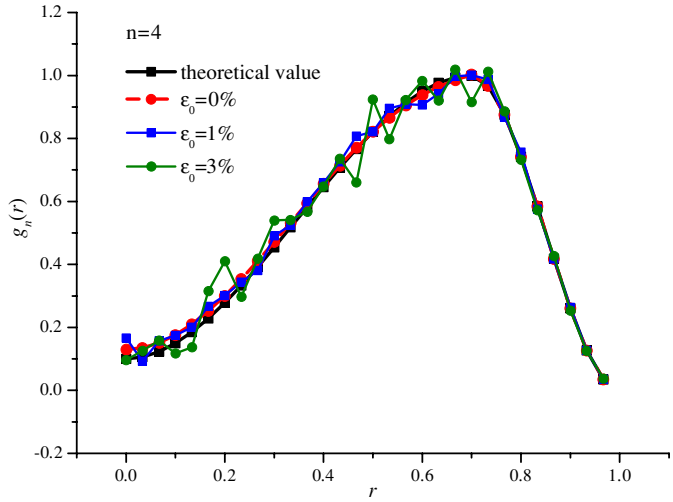

Figure 5. Comparison of the exact emission coefficient $g(r)$ with its fourth-order reconstruction $g_4(r)$ for example 4 (case B) with $\varepsilon_0 = 0\%, 1\%, 3\%$ added noise.

$\sigma = 0.0155$, greater than all values of $\sigma_n (n = 2, \ldots, 5)$ of example 2 in table 2. Furthermore, an inspection of table 2 indicates that two introduced parameters describing the accuracy of reconstruction, σ_n and Δ_n, are consistent.

For case B with random noise, we only consider example 4, and the reason for this selection is that it has the deepest dip at the centre and the reconstructed profile is more susceptible in the presence of noise. In the following computations, we take $n = 3, 4$, and $\varepsilon_0 = 0\%, 1\%, 3\%$, a comparison of $g(r)$ and $g_n(r)$ is plotted in figures 4 and 5 for $n = 3, 4$, respectively. From figures 4 and 5, one can see that the reconstruction is extremely good in

the region of $0.7 < r < 1$, even in the presence of noise. When r goes across the joint-point of the piecewise function, and lies in the region of $0 < r < 0.7$, the reconstructed $g_n(r)$ is also satisfactory, which does not deteriorate the theoretical curve $g(r)$, especially for the vicinity of the $r = 0$. However, for usual techniques for Abel inversion, the reconstructed curve drastically deviates from the theoretical curve near the source centre since the greatest error takes place in the source centre as a consequence of noise propagating from the edge to the source centre [31].

5. Conclusion

This paper presents a novel technique for Abel inversion with noise. The suggested Abel inversion is expressed by the integral of the input data function, and its remarkable advantage is without any artificial smoothing process for raw data. The reconstruction of emission coefficient according to Abel inversion is stable, even for measured radiation intensity $I(y)$ with random noise. An error between Abel inversion and its approximation is analysed. Obtained results for test examples turn out that this method is very effective for measured radiation intensity $I(y)$, even in the case of the presence of noise.

Acknowledgments

The authors would like to give their thanks to two anonymous reviewers for some useful suggestions to improve the original manuscript. This work was partly supported by the National Natural Science Foundation of China under Grant No 10672189.

Appendix

Lemma. *Suppose the matrix*

$$\mathbf{C}_{nn}(x) = \begin{pmatrix} \frac{1}{x} & \frac{1}{x+1} & \cdots & \frac{1}{x+n} \\ \frac{1}{x+1} & \frac{1}{x+2} & \cdots & \frac{1}{x+1+n} \\ \vdots & \vdots & \ddots & \vdots \\ \frac{1}{x+n} & \frac{1}{x+n+1} & \cdots & \frac{1}{x+2n} \end{pmatrix}, \tag{A.1}$$

then for an arbitrary non-negative integer n, the determinant $\det(\mathbf{C}_{nn}(x)) \neq 0$ *for arbitrary positive* x.

Proof. First, by setting $n = 0$ and 1, we can easily get that $\det(\mathbf{C}_{00}(x)) = 1/x$, and $\det(\mathbf{C}_{11}(x)) = [x(2+x)]^{-1} - (1+x)^{-2}$, respectively; so $\det(\mathbf{C}_{00}(x)) \neq 0$, and $\det(\mathbf{C}_{11}(x)) \neq 0$ for $x > 0$.

Second, for $k = n - 1$, one assumes $\det(\mathbf{C}_{n-1,n-1}(x)) \neq 0$. Then for $k = n$, from (A.1) one readily finds

$$\det(\mathbf{C}_{nn}(x)) = \frac{1}{(n+x)\cdots(2n+x)} \begin{vmatrix} \frac{n+x}{x} & \frac{n+x}{x+1} & \cdots & 1 \\ \frac{n+1+x}{x+1} & \frac{n+1+x}{x+2} & \cdots & 1 \\ \vdots & \vdots & \ddots & \vdots \\ \frac{x+2n}{x+n} & \frac{x+2n}{x+n+1} & \cdots & 1 \end{vmatrix}. \tag{A.2}$$

Furthermore, the first n columns subtract the last column, and a further simplification allows us to obtain

$$\det(\mathbf{C}_{nn}(x)) = \frac{1}{n!(n+x)\cdots(2n+x)} \begin{vmatrix} \frac{1}{x} & \frac{1}{x+1} & \cdots & 1 \\ \frac{1}{x+1} & \frac{1}{x+2} & \cdots & 1 \\ \vdots & \vdots & \ddots & \vdots \\ \frac{1}{x+n} & \frac{1}{x+n+1} & \cdots & 1 \end{vmatrix}. \tag{A.3}$$

A similar manipulation for rows can lead to

$$\det(\mathbf{C}_{nn}(x)) = \frac{1}{n!(n+x)^2\cdots(2n-1+x)^2(2n+x)} \begin{vmatrix} \frac{n+x}{x} & \frac{n+x+1}{x+1} & \cdots & 1 \\ \frac{n+x}{x+1} & \frac{n+1+x}{x+2} & \cdots & 1 \\ \vdots & \vdots & \ddots & \vdots \\ 1 & 1 & \cdots & 1 \end{vmatrix}. \tag{A.4}$$

Now, all columns except for the last column subtract the last column, leading to

$$\begin{aligned} \det(\mathbf{C}_{nn}(x)) &= \frac{1}{n!n!(n+x)^2\cdots(2n-1+x)^2(2n+x)} \begin{vmatrix} \frac{1}{x} & \frac{1}{x+1} & \cdots & 1 \\ \frac{1}{x+1} & \frac{1}{x+2} & \cdots & 1 \\ \vdots & \vdots & \ddots & \vdots \\ 0 & 0 & \cdots & 1 \end{vmatrix} \\ &= \frac{1}{n!n!(n+x)^2\cdots(2n-1+x)^2(2n+x)} \det(\mathbf{C}_{n-1,n-1}(x)). \end{aligned} \tag{A.5}$$

Consequently, $\det(\mathbf{C}_{nn}(x)) \neq 0$ for $x > 0$ follows immediately from the assumption of $\det(\mathbf{C}_{n-1,n-1}(x)) \neq 0$ for $x > 0$. Therefore, based on induction we have $\det(\mathbf{C}_{nn}(x)) \neq 0$ for an arbitrary non-negative integer n. □

References

[1] Garcia-Fernandez M, Hernandez-Pajares M, Juan M and Sanz J 2003 *J. Geophys. Res.* **108** 1338
[2] Yoshikawa K and Suto Y 1999 *Astrophys. J.* **513** 549
[3] Munk W and Wunsch C 1983 *Rev. Geophys. Space Phys.* **21** 777
[4] Schreiner W S, Sokolovskiy S V, Rocken C and Hunt D C 1999 *Radio Sci.* **34** 949
[5] Dribinski V, Ossadtchi A, Mandelshtam V A and Reisler H 2002 *Rev. Sci. Instrum.* **73** 2634
[6] Agrawal A K, Albers B W and Griffin D W 1999 *Appl. Optics.* **38** 3394
[7] Hutchinson H 1987 *Principles of Plasma Diagnostics* (New York: Cambridge University Press)
[8] Freeman M P and Katz S 1960 *J. Opt. Soc. Am.* **50** 826
[9] Barr W L 1962 *J. Opt. Soc. Am.* **52** 885
[10] Shimizu T and Horigome T 1989 *Contrib. Plasma Phys.* **29** 307
[11] Maldonado C D, Caron A P and Olsen H N 1965 *J. Opt. Soc. Am.* **55** 1247
[12] Minerbo G N and Levy M E 1969 *SIAM J. Numer. Anal.* **6** 598
[13] Kalal M and Nugent K A 1988 *Appl. Opt.* **27** 1956
[14] Smith L M, Keefer D R and Sudharsanan S I 1988 *J. Quant. Spectorsc. Radiat. Transfer.* **39** 367
[15] Alvarez R, Rodero A and Quintero M C 2002 *Spectrochim. Acta* B **57** 1665
[16] Gottardi N 1979 *J. Appl. Phys.* **50** 2647
[17] Ha J H, Nam Y U, Cheon M S and Hwang Y S 2004 *Rev. Sci. Instrum.* **75** 3408
[18] Chan C K and Lu P 1981 *J. Phys. A: Math. Gen.* **14** 575
[19] Deutsch M and Beniaminy I 1982 *Appl. Phys. Lett.* **41** 27
[20] Anderssen R S and de Hoog F R 1981 *J. Phys. A: Math. Gen.* **14** 3117
[21] Vicharelli P A and Lapatovich W P 1987 *Appl. Phys. Lett.* **50** 557
[22] Gueron S and Deutsch M 1994 *J. Appl. Phys.* **75** 4313
[23] Nestor O H and Olsen H N 1960 *SIAM Rev.* **2** 200

[24] Blades M W and Horlick G 1980 *Appl. Spectrosc.* **34** 696
[25] Hu Q 1996 *SIAM J. Numer. Anal.* **33** 208
[26] Ursell F 1996 *Q. J. Mech. Appl. Math.* **49** 217
[27] Buie M J, Pender J T P, Holloway J P, Vincent T, Ventzek P L G and Brake M L 1996 *J. Quant. Spectorsc. Radiat. Transfer.* **55** 231
[28] Cho Y T and Na S-J 2005 *Meas. Sci. Technol.* **16** 878
[29] Chan G C-Y and Hieftje G M 2006 *Spectrochim. Acta* B **61** 31
[30] Cremer C J and Birkebak R C 1966 *Appl. Opt.* **5** 1057
[31] Ramsey A T and Diesso M 1999 *Rev. Sci. Instrum.* **70** 380

J. Phys. A: Math. Theor. **41** (2008) 049801 (1pp) doi:10.1088/1751-8113/41/4/049801

Corrigendum

A new Abel inversion by means of the integrals of an input function with noise
Li X-F, Huang L and Huang Y 2007 *J. Phys. A: Math. Theor.* 40 347–360

Example 4 given in the paper [1] was mistyped and should read

$$g(r) = \begin{cases} 0.1 + 5.51r^2 - 5.25r^3, & 0 \leqslant r \leqslant 0.7, \\ -40.74 + 155.56r - 188.89r^2 + 74.07r^3, & 0.7 < r \leqslant 1, \end{cases}$$

$$I(y) = \begin{cases} 22.688\,62u^* + 217.557u^*y^2 - 59.49y^4 \ln \dfrac{0.7 + u^*}{y} + 155.56y^2 \ln \dfrac{1+u}{0.7+u^*} + I^*(y), \\ \quad 0 \leqslant r \leqslant 0.7 \\ I^*(y) + 155.56y^2 \ln \dfrac{1+u}{y}, \qquad 0.7 < r \leqslant 1, \end{cases}$$

with

$$I^*(y) = -14.811\,667u - 196.300\,83uy^2 + 55.5525y^4 \ln \frac{1+u}{y}$$

The authors apologize for any inconvenience. However, the authors would like to assure readers that these are merely misprints and as such do not affect the results presented in the paper [1] since they were evaluated and compared according to the above correct version.

References

[1] Li X-F, Huang L and Huang Y 2007 *J. Phys. A: Math. Theor.* **40** 347

1751-8113/08/049801+01$30.00